Proceedings of the 10th International Conference of Control Systems, and Robotics (CDSR'23)
Ottawa, Canada – June 01 - 03, 2023
Paper No. 204
DOI: 10.11159/cdsr23.204

Control the Quadcopter using Hybrid Controller under the Disturbed Environment

Sanjay Kumar[1], Lillie Dewan[2]
[1,2]National Institute of Technology Kurukshetra
Kurukshetra, Haryana, India

Abstract **-** This paper aims to propose a robust nonlinear control for quadcopter autonomous flight control that improves the tracking control for quadcopters under disturbances and the wind effect. The quadcopter dynamics contain uncertainties, external disturbances, mass variation (parametric uncertainty), and wind effect. Hybrid SMCBS with proportional-fractional order- integral-derivative controller (PFOID) surface is proposed to mitigate the effect of disturbances. The stability is proved of the system with a proposed controller with the help of the Lyapunov Stability criterion, which guarantees that all states retain and reach the sliding surface. A quadcopter's tracking control problem is investigated using linear motion and a helix structure (trajectories). To validate the performance of PFOIDSMCBS, it has been implemented on the quadcopter models. The proposed controller's performance is evaluated and compared with (PID-SMC) and (SMC-BS) and ability to mitigate the effects of the disturbances. It is observed that the system is stable as it satisfies the stability condition derived using the Lyapunov stability criterion, and successfully tracks a given reference in a noisy environment.

Keywords**:** Backstepping controller, Hybrid controller, Nonlinear system, Sliding Mode controller, Proportional-Integral-Derivative, Quadcopter Model.

1. Introduction

Quadcopter UAVs have been widely used in various applications due to their numerous advantages [1] [2]. In industrial and academic applications, robust trajectory tracking control has become an important topic to achieve high performance, fast response time, high robustness, and accuracy in autonomous flight missions. In flight control, the angular and translational motion factors are highly nonlinear and strongly linked, and their behavior affects the stability and safety of the flight mission [3].

Researchers have recently researched UAVs, including the control algorithm for controlling the quadcopter [4][5]. Several linear and nonlinear control methods have been applied [6]. SMC and BS have gained attention due to their capacity to provide stability, disturbance rejection, and robustness [7][8]. The classical and modified backstepping control approach has been represented in [9]. SMC is the most efficient and robust control method because it is insensitive to model errors and system parameter variations [10]. An integral SMC [11] and an integral backstepping SMC have been proposed to deal with the quadcopter's robust trajectory tracking.

Extending the SMC method [12][13] improves the performance under external disturbances and removes the chattering effect. Various hybrid controller has been proposed to achieve the desired trajectory and mitigate the effect of the disturbances like SMCBS [14] and PIDSMC [15], PFOIDSMC [16], and PIDSMCBS [17].

The literature shows that different nonlinear control schemes tackle the aerodynamic effect, senor noise, wind effect, and payload considered individually. This paper proposes a hybrid controller (proportional fractional-order integral derivative surface-based SMC with BS) to track the trajectory considering all the disturbances. The performance of the proposed control has been compared with existing controllers SMCBS [14], and PIDSMC [15]. Stability is proved with the help of the Lyapunov criterion. Simulation has been done with three quadcopter models.

The paper is structured as follows: Section 2 discusses the quadcopter's dynamics. Proposed controller and stability conditions are derived in section 3 and implemented in Section 4, Section 5 followed by conclusions.

2. Mathematical Model

The quadcopter model has been described in [17] is shown in Figure 1.

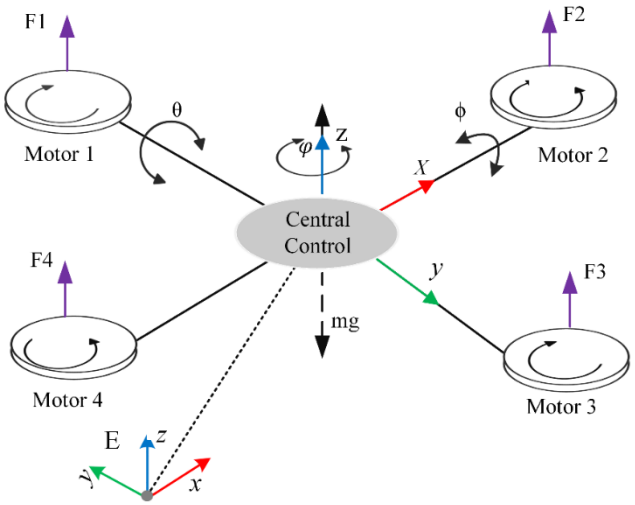

Fig. 2: Control scheme diagram

Figure 1 represents the position of the center of mass of the quadcopter in $x, y,$ and z direction, relative to the earth fixed frame E. Rotational angles are; roll, pitch, and yaw around the x, y, and z-axis, respectively. State space representation of model [17].

$$\dot{\mathrm{A}} = f(\mathrm{A}, u) + d(\mathrm{A}, u) \tag{1}$$

State vector is the A, d is the disturbances vector, and u is the input vector.

$$\mathrm{A} = \begin{vmatrix} \mathrm{A}_1 = \phi, \mathrm{A}_2 = \dot{\phi}, \mathrm{A} = \theta, \mathrm{A} = \dot{\theta}, \\ \mathrm{A}_5 = \varphi, \mathrm{A}_6 = \dot{\varphi}, \mathrm{A}_7 = z, \mathrm{A} = \dot{z}, \\ \mathrm{A}_9 = x, \mathrm{A}_{10} = \dot{x}, \mathrm{A}_{11} = y, \mathrm{A}_{12} = \dot{y}, \end{vmatrix} \epsilon R^{12} \tag{2}$$

$$u = \left|u_{\phi}, u_{\theta}, u_{\varphi}, u_z\right|'$$

$$\dot{\mathrm{A}} = \begin{cases} \dot{\mathrm{A}}_1 = \mathrm{A}_2 \\ \dot{\mathrm{A}}_2 = J_{xx}^{-1}\left((J_{yy} - J_{zz})\dot{\theta}\dot{\varphi} + J_r\dot{\theta}\bar{n}\right) + b_1 u_\phi + d_{ro\phi} \\ \dot{\mathrm{A}}_3 = \mathrm{A}_4 \\ \dot{\mathrm{A}}_4 = J_{yy}^{-1}\left((J_{zz} - J_{xx})\dot{\varphi}\dot{\phi} - J_r\dot{\phi}\bar{n}\right) + b_2 u_\theta + d_{ro\theta} \\ \dot{\mathrm{A}}_5 = \mathrm{A}_6 \\ \dot{\mathrm{A}}_6 = J_{zz}^{-1}\left((J_{xx} - J_{yy})\dot{\theta}\dot{\phi}\right) + b_3 u_\varphi + d_{ro\varphi} \\ \dot{\mathrm{A}}_7 = \mathrm{A}_8 \\ \dot{\mathrm{A}}_8 = g - m^{-1}\chi_z u_z + d_{trz} \\ \dot{\mathrm{A}}_9 = \mathrm{A} \\ \dot{\mathrm{A}}_{10} = m^{-1}\chi_x u_x + d_{trx} \\ \dot{\mathrm{A}}_{11} = \mathrm{A}_{12} \\ \dot{\mathrm{A}}_{12} = g - m^{-1}\chi_y u_y + d_{try} \end{cases} \quad (3)$$

Where $b_1 = \frac{l}{J_{xx}}$, $b_2 = \frac{l}{J_{yy}}$, $b_3 = \frac{l}{J_{zz}}$, $\chi_x = c\phi s\theta c\varphi + s\phi s\varphi, \chi_y = c\phi s\theta s\phi - s\phi c\varphi, \chi_z = c\phi c\theta$

2.1. Disturbance model

The mathematical representation of various disturbances [17] considered acting on the system is:

- Aerodynamic moment d_i^{ae}= sin(2t)
- Sensor noise d_i^{sn}= used 'rand,' function in Matlab, the value lie between 0 and 1.
- External noise d_i^{ae}=

$$\left.\begin{array}{c} nd_\phi^{en}(t) = nd_\theta^{en}(t) = 7 + 2\cos\left(\frac{2\pi}{3}t\right) \\ nd_\varphi^{en}(t) = 5 + 2\cos\left(\frac{\pi}{2}t\right) \\ nd_x^{en}(t) = nd_y^{en}(t) = nd_z^{en}(t) = 18 + 4\cos\left(\frac{\pi}{6}t\right) \end{array}\right\} t = 0.01sec$$

- Wind noise d_i^w [17] acts as a shock on the quadcopter with the speed of 3 m\s, after 8 seconds act in trajectory-1, and after 25 seconds act in trajectory-2 with the same speed.
- Total disturbance in translation d_{tri} and rotational d_{roi} motion is;

$$\left.\begin{matrix} d_{tri} \\ d_{roi} \end{matrix}\right\} = d_i^{ae} + d_i^{sn} + d_i^{en} + d_i^w + d_i^{PU} \quad (4)$$

Other quadcopter model parameters/variables with their values are defined in Table 1.

Table 1: Physical parameters

Variable	Definition	Value/ Unit [18]
m	mass	1.12 kg
g	gravity	9.8 m/s^2
l	Arm length	0.23 m
R	Radius of the propellers	-
$J_{xx} = J_{yy}$	Inertia on x, y axis	0.0119 kg.m^2
J_{zz}	Inertia on z-axis	0.0223 kg.m^2
l_f	left coefficient	7.73213×(10^{-6}) Ns^2
J_r	Rotor inertia	8.5×(10^{-4}) kg.m^2
k_f and k_m	Aerodynamic forces and moment constant	3.13e^{-5} Ns^2 and 7.5e-5 Nms^2

3. Control Design

The quadcopter dynamics are underactuated and nonlinear with the 6 output $(x, y, z, \phi, \theta, \varphi)$ variables and 4 control inputs $(u_z, u_\phi, u_\theta, u_\varphi)$. The control schemes diagram is shown below (Figure 2).

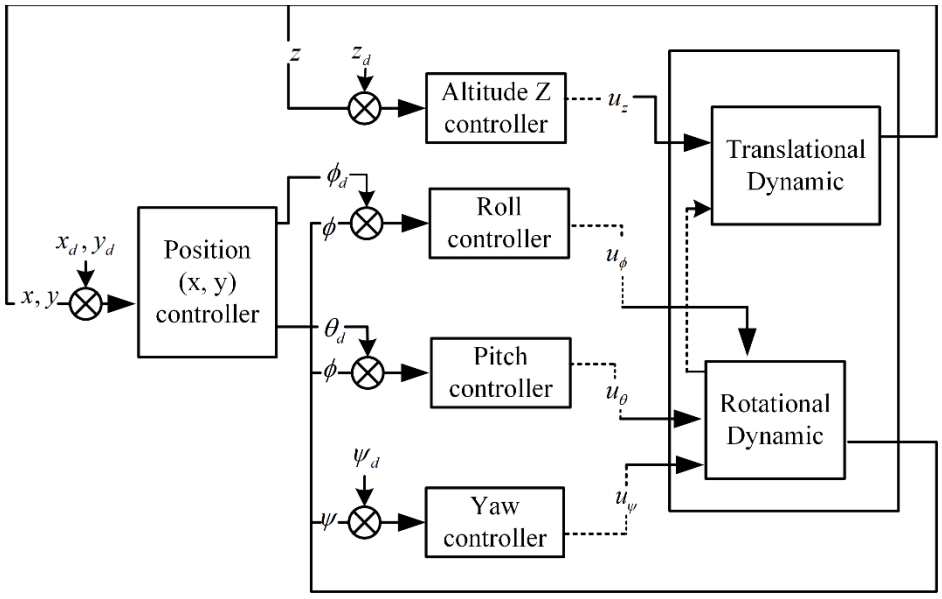

Fig. 2: Control scheme diagram

General SMC control law is,

$$u_i^+ = u_E + u_S \tag{5}$$

(u_E) is the control signal without external disturbances and linearization of the input/output. (u_S) the switching control law, provides additional control effort for disturbances and reduces tracking error.

3.1 PFOIDSMCBS controller

3.1.1 SMC with BS

The tracking error (z_{ri}) for SMC with BS is [17][19];

$$z_{ri} = \xi_{id} - \xi_i$$
$$\dot{z}_{ri} = \dot{\xi}_{id} - \xi_i - \eta_i \varepsilon_i \text{ with } 0 < \eta_i < \infty \tag{6}$$

and

$$\ddot{z}_{ri} = \ddot{\xi}_{id} - \dot{\xi}_i - \eta_i \dot{\varepsilon}_i,\ i = \phi, \theta, \varphi, z, x, y$$

In the design, considered the PFOID as a sliding surface: to drive PFOID first take PID surface [17], [20] and converting it into the PFOID;

$$\dot{s}_i + \gamma_i s_i = k_{pi} z_{ri} + k_{ii} \int_0^t z_{ri} dt + k_{di} \dot{z}_{ri}$$
$$\ddot{s}_i + \gamma_i \dot{s}_i = k_{pi} \dot{z}_{ri} + k_{ii} z_{ri} dt + k_{di} \ddot{z}_{ri},\ \ \gamma_i\ \varepsilon R^+ \tag{7}$$

$$\ddot{s}_i + \gamma_i \dot{s}_i = k_{pi} \dot{z}_{ri} + k_{ii}^a z_{ri} dt + k_{di}^b \ddot{z}_{ri} \tag{8}$$

Firstly, the calculation for roll:

By using the Eq. (6), calculating the value $\ddot{z}_{r\phi}$ is;

$$\ddot{z}_{r\phi} = \ddot{\xi}_{\phi d} - \dot{\xi}_\phi - \eta_\phi \dot{\varepsilon}_1$$
$$\ddot{z}_{r\phi} = \ddot{\xi}_{\phi d} - \left(\frac{(J_{yy} - J_{zz})}{J_{xx}} \dot{\theta}\dot{\varphi} + \frac{J_r}{J_{xx}} \dot{\theta}\bar{n} + b_1 u_\phi + d_{ro\phi} \right) - \alpha_\phi (\varepsilon_1 + \eta_\phi \varepsilon_1) \tag{9}$$

So, the sliding surface Eq. (8) in the term of roll input;

$$\ddot{s}_\phi + \gamma_\phi \dot{s}_\phi = k_{p\phi} \dot{z}_{r\phi} + k_{i\phi}^a z_{r\phi} dt + k_{d\phi}^b \ddot{z}_{r\phi} \tag{10}$$

Substituted the Eq. (9) into (10)

$$\ddot{s}_\phi + \gamma_\phi \dot{s}_\phi = k_{p\phi} \dot{z}_{r\phi} + k_{i\phi}^a z_{r\phi} + k_{d\phi}^b \left(\ddot{\xi}_{\phi d} - \left(\frac{(J_{yy} - J_{zz})}{J_{xx}} \dot{\theta}\dot{\varphi} + \frac{J_r}{J_{xx}} \dot{\theta}\bar{n} + b_1 u_\phi + d_{ro\phi} \right) - \alpha_\phi (\varepsilon_1 + \eta_\phi \varepsilon_1) \right) \tag{11}$$

$\ddot{s}_\phi = 0$ for tracking error to remain on the sliding surface and external disturbance is zero $d_{ro\phi} = 0$;

$$u_E = u_\phi = \frac{1}{b_\phi k_{d\phi}^b}\left(-\gamma_\phi \dot{s}_\phi + k_{p\phi}\dot{z}_{r\phi} + k_{i\phi}^a z_{r\phi} + k_{d\phi}^b\left(\ddot{\xi}_{\phi d} - \left(\frac{(J_{yy}-J_{zz})}{J_{xx}}\dot{\theta}\dot{\varphi} + \frac{J_r}{J_{xx}}\dot{\theta}\bar{n}\right) - \alpha_\phi\left(\varepsilon_2 + \eta_\phi \varepsilon_1\right)\right)\right) \tag{12}$$

The switching function introduced is;

$$u_s = \lambda_i s_i + k_i sign(\dot{s}_i), \;\; \lambda_i, k > 0 \tag{13}$$

For sign function [21] defined as;

$$sign(s_i) = \begin{cases} +1, if\ \dot{s(t)} > 0 \\ 0 \;\; if\ \dot{s(t)} = 0 \\ -1 \;\; if\ \dot{s(t)} < 0 \end{cases}$$

Using approaches [22] and [23], the roll input equation is calculated by substituting Eq. (11) and (12) into (5).

$$u_\phi = \frac{1}{b_\phi k_{d\phi}^b}\left(-\gamma_\phi \dot{s}_\phi + k_{p\phi}\dot{z}_{r\phi} + k_{i\phi}^a z_{r\phi} + k_{d\phi}^b\left(\left(\ddot{\xi}_{\phi d} - \left(\frac{\left(J_{yy}-J_{zz}\right)}{J_{xx}}\dot{\theta}\dot{\varphi} + \frac{J_r}{J_{xx}}\dot{\theta}\bar{n}\right) - \eta_\phi^2 \varepsilon_1\right) + \lambda_\phi s_\phi + k_\phi sign(\dot{s}_\phi)\right)\right) \tag{14}$$

So, $\ddot{s}_\phi$ is calculated by substituting the Eq. (14) into the Eq. (12)

$$\ddot{s}_\phi = -k_{d\phi}^b d_{ro\phi} - b_\phi k_{d\phi}^b \lambda_\phi s_\phi - b_\phi k_{d\phi}^b k_\phi sign(\dot{s}_\phi) \tag{15}$$

And modifying the surface Eq. (15) in a generalized form;

$$\ddot{s}_i = -k_{di}^b d_{roi} - b_i k_{di}^b \lambda_i s_i - b_i k_{di}^b k_i sign(\dot{s}_i) \tag{16}$$

Now, the roll input with the disturbance is;

$$u_{\phi}^{+}=\frac{1}{b_{\phi}k_{d\phi}^{b}}\Bigg(-\gamma_{\phi}\dot{s}_{\phi}+k_{p\phi}\dot{z}_{r\phi}+k_{i\phi}^{a}z_{r\phi} + k_{d\phi}^{b}\Bigg(\Bigg(\ddot{\xi}_{\phi d}-\Bigg(\frac{\left(J_{yy}-J_{zz}\right)}{J_{xx}}\dot{\theta}\dot{\varphi}+\frac{J_{r}}{J_{xx}}\dot{\theta}\bar{n}+d_{ro\phi}\Bigg)-\eta_{\phi}^{2}\varepsilon_{1}\Bigg) +\lambda_{\phi}s_{\phi}+k_{\phi}sign\left(\dot{s}_{\phi}\right)\Bigg)\Bigg)\Bigg) \tag{17}$$

Other control inputs for rotational and translational subsystems calculated on the same line are defined as;

$$u_{\theta}^{+}=\frac{1}{b_{\theta}k_{d\theta}^{b}}\Bigg(-\gamma_{\theta}\dot{s}_{\theta}+k_{p\theta}\dot{z}_{r\theta}+k_{i\theta}^{a}z_{r\theta} + k_{d\theta}^{b}\Bigg(\Bigg(\ddot{\xi}_{\theta d}-\Bigg(\frac{\left(J_{zz}-J_{xx}\right)}{J_{yy}}\dot{\varphi}\dot{\phi}-\frac{J_{r}}{J_{yy}}\dot{\phi}\bar{n}+d_{ro\theta}\Bigg)-\eta_{\theta}^{2}\varepsilon_{3}\Bigg) +\lambda_{\theta}s_{\theta}+k_{\theta}sign(\dot{s}_{\theta})\Bigg)\Bigg)\Bigg) \tag{18}$$

$$u_{\varphi}^{+}=\frac{1}{b_{\varphi}k_{d\varphi}^{b}}\Bigg(-\gamma_{\varphi}\dot{s}_{\varphi}+k_{p\varphi}\dot{z}_{r\varphi}+k_{i\varphi}^{a}z_{r\varphi} + k_{d\varphi}^{b}\Bigg(\Bigg(\ddot{\xi}_{\varphi d}-\Bigg(\frac{\left(J_{xx}-J_{yy}\right)}{J_{zz}}\dot{\phi}\dot{\theta}+d_{ro\varphi}\Bigg)-\eta_{\theta}^{2}\varepsilon_{5}\Bigg)+\lambda_{\phi}s_{\varphi}+k_{\varphi}sign\left(\dot{s}_{\varphi}\right)\Bigg)\Bigg) \tag{19}$$

with

$$\begin{cases}\varepsilon_{3}=\xi_{\theta d}-\xi_{\theta},s_{\theta}=\varepsilon_{4}=\dot{\xi}_{\theta d}-\xi_{\theta}-\eta_{\theta}\varepsilon_{3}, & for\ pitch\\ \varepsilon_{5}=\xi_{\varphi d}-\xi_{\varphi},s_{\varphi}=\varepsilon_{6}=\dot{\xi}_{\varphi d}-\xi_{\varphi}-\eta_{\varphi}\varepsilon_{5}, & for\ yaw\end{cases}$$

$$u_{z}^{+}=\frac{m}{\chi_{z}}k_{pz}\dot{z}_{rz}+k_{iz}^{a}z_{rz}+k_{dz}^{b}\left(\ddot{\xi}_{zd}-(g+d_{trz})-\eta_{z}^{2}\varepsilon_{7}+\lambda_{z}s_{z}+k_{z}sign(\dot{s}_{z})\right) \tag{20}$$

with

$$\varepsilon_{7}=\xi_{zd}-\xi_{z},s_{z}=\varepsilon_{8}=\dot{\xi}_{zd}-\xi_{z}-\eta_{z}\varepsilon_{7}$$

$$u_{x}^{+}=\frac{m}{\chi_{x}}k_{px}\dot{z}_{rx}+k_{ix}^{a}z_{rx}+k_{dx}^{b}\left(\ddot{\xi}_{xd}-(d_{trx}-\eta_{x}^{2}\varepsilon_{9})+\lambda_{x}s_{x}+k_{x}sign(\dot{s}_{x})\right) \tag{21}$$

$$u_y^+ = \frac{m}{\chi_y} k_{py}\dot{z}_{ry} + k_{iy}^a z_{ry} + k_{dy}^b \left(\ddot{\xi}_{yd} - d_{trz} - \eta_y^2 \varepsilon_{11} + \lambda_y s_y + k_y sign\left(\dot{s}_y\right)\right) \tag{22}$$

with

$$\begin{cases} \varepsilon_9 = \xi_{xd} - \xi_{x,}\ s_x = \varepsilon_{10} = \dot{\xi}_{xd} - \xi_x - \eta_x \varepsilon_9, \ \ for\ x \\ \varepsilon_{11} = \xi_{yd} - \xi_{y,}\ s_y = \varepsilon_{12} = \dot{\xi}_{yd} - \xi_y - \eta_y \varepsilon_{11}, \ \ for\ y \end{cases}$$

3.2. Stability Analysis

Quadcopter sliding surface given by Eq. (8) and control law $\left(u_{z,} u_{\phi,} u_{\theta,} u_{\varphi}\right)$ defined by Eq. (17,18,19,20) is asymptotically stable if : $\dot{V}_i < 0$ (is negative definite) for differential quadratic Lyapunov function [17] [24] defined as;

$$\dot{V} = s_i \dot{s}_i + \dot{s}_i \ddot{s}_i \tag{23}$$

Proof 1: for roll, pitch and yaw; using Eq. (23) and substituting the value $\ddot{s}_i$ defined in Eq. (16);

$$\begin{aligned} &= s_i \dot{s}_i + \dot{s}_i \left(-k_{di}^b d_{roi} - b_i k_{di}^b \lambda_i s_i - b_i k_{di}^b k_i sign(\dot{s}_i)\right) \\ &= \dot{s}_i \left(s_i - k_{di}^b d_{roi} - b_i k_{di}^b \lambda_i s_i - b_i k_{di}^b k_i |\dot{s}_i|\right) \\ &\leq |\dot{s}_i| \left(s_i - k_{di}^b d_i - b_i k_{di}^b \lambda_i s_i - b_i k_{di}^b k_i |\dot{s}_i|\right) \\ &\leq |\dot{s}_i| \left(s_i \left(1 - b_i k_{di}^b \lambda_i\right) + k_{di}^b \left(d_{roi}^+ - b_i k_{di}^b\right) |\dot{s}_i|\right) \end{aligned}$$

Where $d_i^+ \in R$ is the upper bound on disturbance [18]. For asymptotic stability $\dot{V}_i < 0$, and negative if:

$$\begin{cases} \lambda_i > \dfrac{1}{b_i k_{di}^b} \\ k_i > \dfrac{d_{roi}^+}{b_i} \end{cases} where\ i = \phi, \theta, \varphi \tag{24}$$

Proof 2: for z

Using the Eq. (22) substituting the value define as $\ddot{s}_z$, calculated as same way as $\ddot{s}_\phi$.

$$\ddot{s}_5 = -k_{dz}^b d_z - k_{dz}^b \lambda_z s_z - k_{dz}^b k_z sign(\dot{s}_z)$$

$$\begin{aligned} \dot{V} &= s_z \dot{s}_z + \dot{s}_z \ddot{s}_z \\ &= s_z \dot{s}_z + \dot{s}_z \left(-k_{dz}^b d_z - k_{dz}^b \lambda_z s_z - k_{dz}^b k_z sign(\dot{s}_z)\right) \end{aligned}$$

$$= \dot{s}_z\left(s_z - k_{dz}^b d_z - k_{dz}^b \lambda_z s_z - k_{dz}^b k_z |\dot{s}_z|\right)$$
$$\leq |\dot{s}_z|\left(s_z - k_{dz}^b \lambda_z s_z - k_{dz}^b d_z - k_{dz}^b k_z |\dot{s}_z|\right)$$
$$\leq |\dot{s}_z|\left(s_z\left(1 - k_{dz}^b \lambda_z\right) + k_{dz}^b (d_{trz}^+ - k_z)|\dot{s}_z|\right)$$

$\dot{V}$ it will always be negative if:

$$\left.\begin{aligned} \lambda_z &> \frac{1}{k_{dz}^b} \\ k_z &> d_{trz}^+ \end{aligned}\right\} \tag{25}$$

4. Simulation Result

The proposed controller has been implemented on the quadcopter models to follow the desired trajectory 1 and 2 (Figure 3) in MATLAB/Simulink version 2021b. The transient response has been compared with the existing (i) SMCBS [14] and (ii) PIDSMC [15] controllers under disturbances and parametric uncertainties. Graphical results of controllers are presented for clarity of graphs and quantified in Tables.

For the quadcopter parameters defined in Table 1, PID gains are determined using the ultimate gain method, and sliding function gains tuned by the hit and trial method are listed in Table 2. Fractional power chosen for Integrator (I) a=0.8, Derivative (D) b=0.65.

4.1. Trajectory

Trajectory-1, the initial and final values of position are (0,0,0) meters and (1,1,1) meters, and angle values are (0,0,0) radians and (0,0,0) radians, respectively. The quadcopter takes off at 0 sec and flies over 15 seconds. After the 8th-second oscillation is observed due to wind disturbance, the system settles slowly. Figures 4 show the performance of the controller's responses. Trajectory-2 is a helix structure are shown in Figure5.

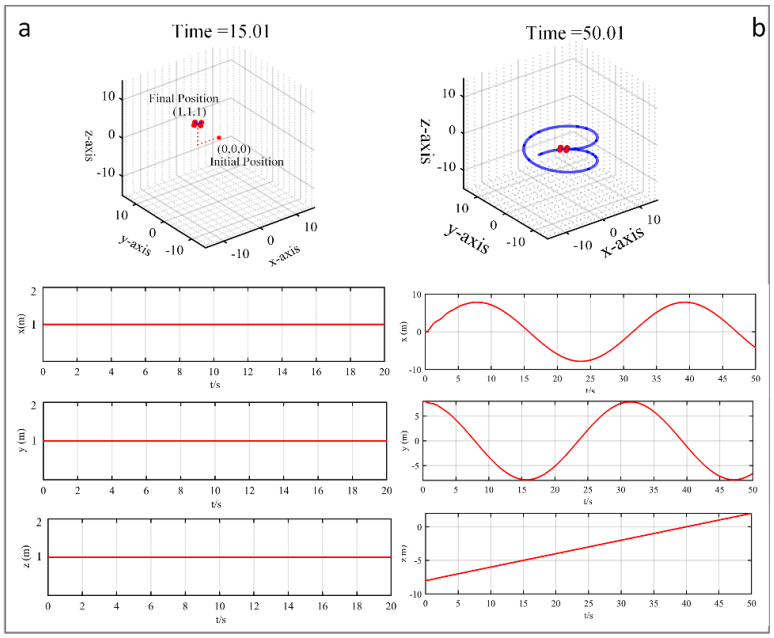

Fig. 3: Trajectory 1) Linear motion 2) Helix structure

Table. 2. Controller parameters

Variables	x	y	z	$\emptyset$	θ	φ
k_p	5.5	6.0	10.0	9.0	9.0	8.0
k_i	0.86	0.86	1.05	1.24	1.36	0.88
k_D	0.66	0.66	0.11	0.33	0.33	0.13
λ_i	2.0	2.0	2.0	1.0	1.0	3.0
k_i	20.0	20.0	20.0	19.0	19.0	20.0

4.1.1 Trajectory 1

The quadcopter takes off at 0 seconds from the 0.0 m. The proposed controller takes 2.94 seconds to reach 1.0 m. After the 8th second, oscillation observed due to the wind settles slowly to its original trajectory in 3.03 seconds. The results are quantified in Table 3 and compared with the SMCBS and PIDSMC controllers.

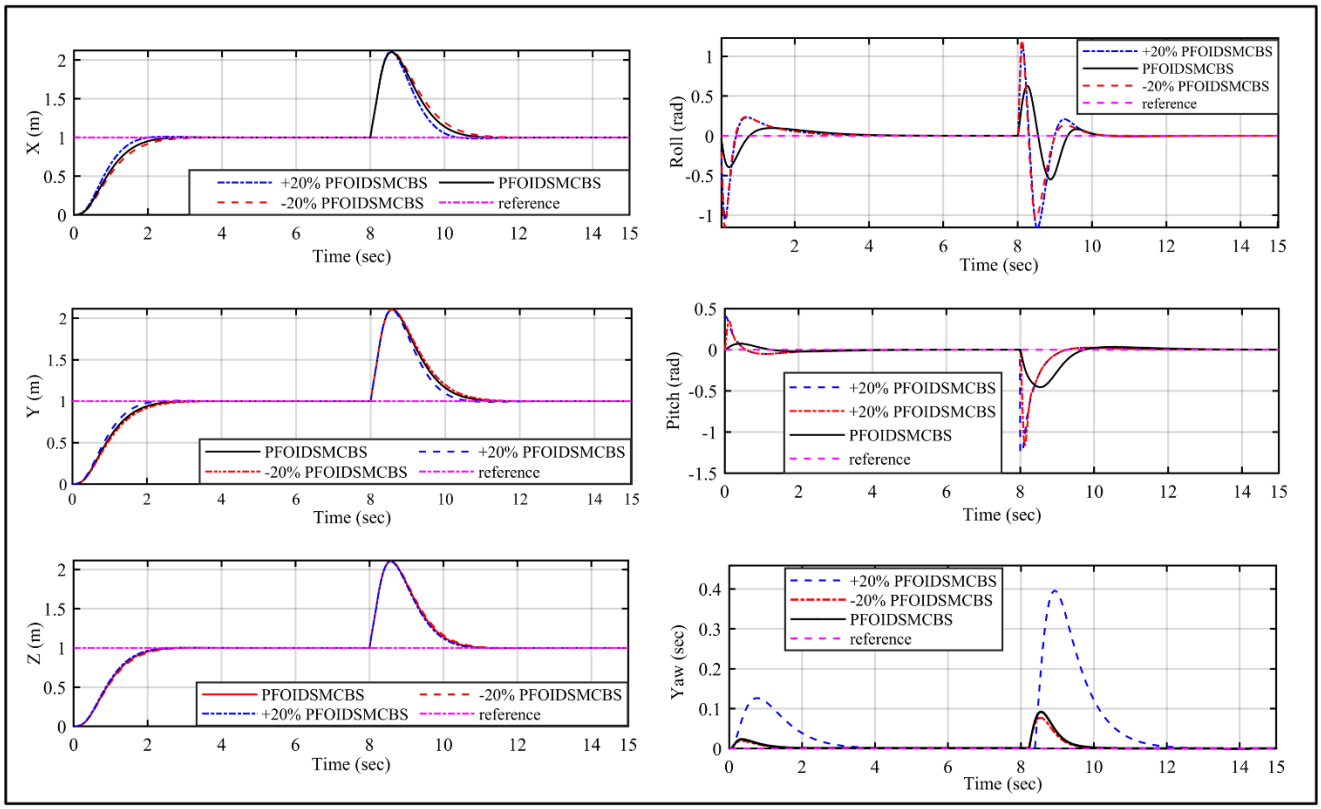

Fig. 4: Performance comparision of the existing and proposed controller.

4.2. Trajectory-2 Helix structure

The effectiveness of controllers' is tested when the quadcopter tracks a helical trajectory [17] for a time interval of 0-50 seconds. The effect of wind disturbance at a speed of 3m/s is added to the system from the 25th second. The proposed controller can mitigate the effect of disturbances and wind disturbances. Figure 5 show that the proposed controller exhibits good performance versus the existing controllers. The RMSE value with PFOIDSMCBS (z-direction) is observed from Table 4

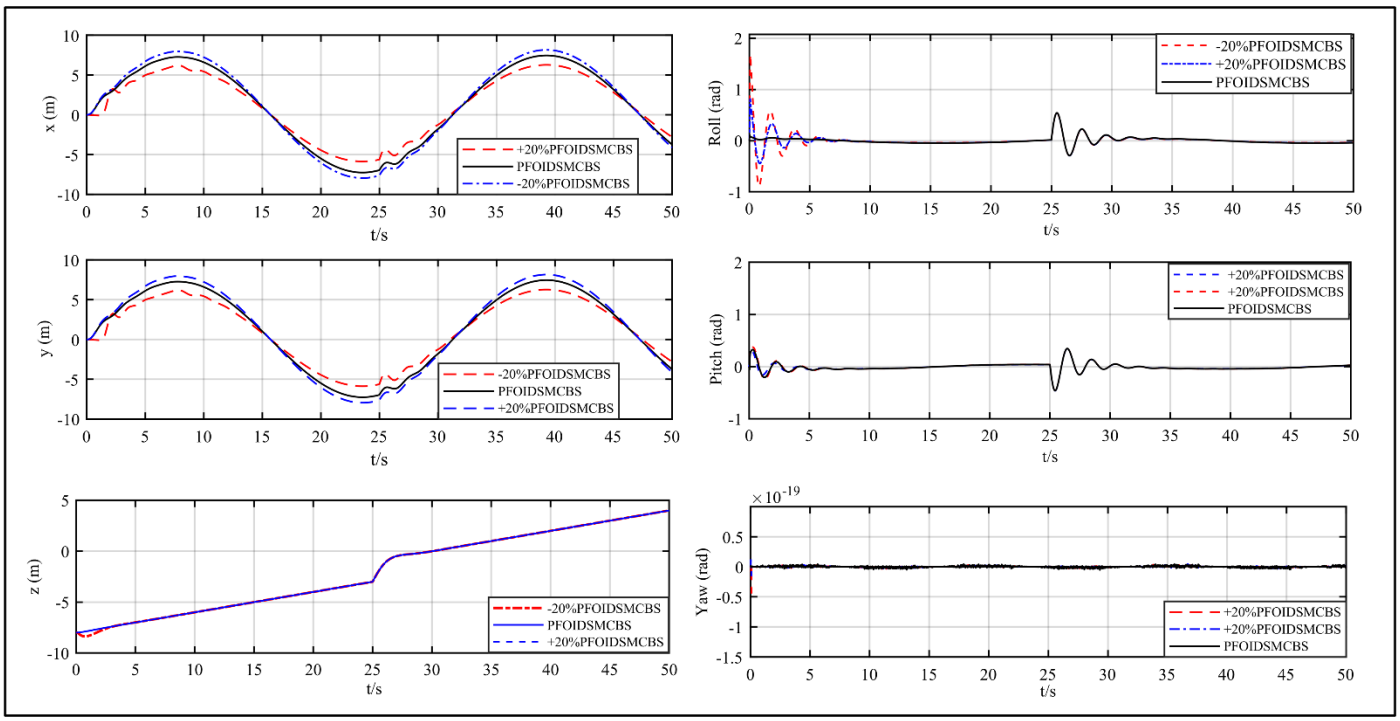

Fig. 5: Performance comparision of the existing and proposed controller

Table. 3. Performance specification of the test 1 (Trajectory-1)

Parameters			x	y	z	$\emptyset$	θ	φ
Rise time	SMCBS	No Wind effect	2.33	2.33	2.27	0.90	0.72	0.73
	PIDSMC	No Wind effect	2.15	2.25	2.12	0.55	0.72	0.67
	PFOID SMCBS	No Wind effect	1.73	1.73	1.71	0.180	1.27	1.74
		No wind effect +20% (PU)	1.42	1.42	1.65	0.41	0.59	1.78
		No Wind effect -20% (PU)	1.89	1.89	1.79	0.41	0.59	1.78
Overshoot Time	SMCBS	No wind effect	0	0	0	-1.16	0.44	0.13
		Wind effect	2.18	2.18	2.18	1.25	-1.26	0.51
	PIDSMC	No wind effect	0	0	0	-1.06	0.45	0.12
		Wind effect	2.12	2.12	2.12	1.12	-1.21	0.07
	PFOID SMCBS	No wind effect	0	0	0	-0.39	0.07	0.02
		Wind effect	2.10	2.10	2.10	0.54	-0.45	0.09
		No wind effect +20% (PU)	0	0	0	-1.06	0.39	0.126
		Wind effect +20% (PU)	2.01	2.01	2.01	1.14	-1.24	0.39
		No wind effect -20% (PU)	0	0	0	-1.03	0.33	0.02
		Wind effect -20% (PU)	2.10	2.10	2.10	1.03	-1.14	0.07
Settling Time	SMCBS	No wind effect	3.21	3.21	3.18	4.42	4.21	3.91
		Wind effect	12.04	12.04	11.91	11.22	12.23	10.56
	PIDSMC	No wind effect	3.14	3.14	3.12	4.28	3.20	3.81
		Wind effect	11.58	11.58	11.44	11.01	11.88	10.40
	PFOID	No wind effect	3.01	3.01	2.94	4.21	4.01	3.74

	SMCBS	Wind effect	11.04	11.04	11.03	10.30	12.01	10.33
		No Wind effect +20% (PU)	2.34	2.34	2.07	4.07	3.01	1.78
		Wind effect +20% (PU)	10.41	10.41	10.20	10.20	11.58	12.06
		No wind effect -20% (PU)	3.34	3.34	3.29	4.21	3.01	1.78
		Wind effect -20% (PU)	11.61	11.61	11.31	10.40	11.58	10.33
Steady State Error	SMCBS	No wind effect	0	0	0	0.001	-0.006	0.001
		Wind effect	0.004	0.004	0.004	0.002	0.014	0.004
	PIDSMC	No wind effect	0.001	0.001	0.001	0.001	-0.005	0.001
		Wind effect	0.013	0.013	0.003	0.001	-0.006	0.001
	PFOID SMCBS	No wind effect	0	0	0	0.001	-0.006	0.001
		Wind effect	0.004	0.004	0.004	0.002	0.014	0.004
		No wind effect +20% (PU)	0.001	0.001	0.001	0.001	-0.005	0.001
		Wind effect +20% (PU)	0.013	0.013	0.003	0.002	0.004	0.013
		No wind effect -20% (PU)	0.004	0.004	0.004	0.004	-0.005	0.004
		Wind effect -20% (PU)	0.005	0.005	0.005	0.005	0.004	0.005

Table. 4. RMSE value (Trajectory-2)

Controllers	x	y	z	$\emptyset$	θ	φ
PIDSMC	1.360	1.388	0.415	0.338	0.553	$1.19e^{-6}$
SMCBS	0.599	0.567	0.394	0.238	0.199	$1.13\ e^{-6}$
PFOIDSMCBS	0.389	0.188	0.299	0.105	0.082	$1.25\ e^{-6}$

Table. 5. Stability Analysis

Parameters and values	$\lambda_\emptyset = 20$	$\lambda_\theta = 20$	$\lambda_\varphi = 20$	$\lambda_z = 20$	$k_\emptyset = 2.26$	$k_\theta = 2.56$	$k_\varphi = 3.20$	$k_z = 3.69$
Parameters and values	$\frac{1}{b_\emptyset k_{d\emptyset}^b} = 3.78$	$\frac{1}{b_\theta k_{d\theta}^b} = 3.78$	$\frac{1}{b_\varphi k_{d\varphi}^b} = 5.56$	$\frac{1}{k_{dz}^b} = 1.25$	$\frac{d_{ro\emptyset}^+}{b_\emptyset} = 0.71$	$\frac{d_{ro\theta}^+}{b_\theta} = 0.57$	$\frac{d_{ro\varphi}^+}{b_\varphi} = 2.35$	$d_{trz}^+ = 1.67$

In the RMSE value of PFOIDSMCBS is 27.9% less than SMCBS and 31.7% less than PIDSMC. Therefore, proposed controller outperforms another controller with a small error.

4.1. Stability Analysis

From Eq. (24) and (25), conditions for asymptotically stability are:

$$\begin{Bmatrix} \lambda_i > \frac{1}{b_i k_{di}^b} \\ k_i > \frac{d_{roi}^+}{b_i} \end{Bmatrix} \; where\ i = \phi, \theta, \varphi \qquad \begin{Bmatrix} \lambda_z > \frac{1}{k_{dz}^b} \\ k_z > d_{trz}^+ \end{Bmatrix} \text{ for z}$$

Table 5 shows that the stability conditions are fulfilled, implying that the system is asymptotically stable.

5. Conclusion

A simple hybrid controller (PFOIDSMCBS) is proposed to improve a quadcopter's attitude, altitude, and angle tracking tracking performance. The proposed controller can be deployed with quadcopters in the presence of various disturbances (external disturbances, wind effects, and mass variation) during flight state. To demonstrate the effectiveness and robustness robustness of the controllers has been compared with the PIDSMC and SMCBS controllers. Performances have been done on the linear and helical trajectories under the disturbances. Simulation results shown that the proposed controller has successfully tracked the quadcopter movement to desired/reference values for trajectories 1 and 2, ensuring the system's stability. Optimizing the controller parameters and power can improve the controller's tracking capability.

References

[1] K. Alexis, G. Nikolakopoulos, A. Tzes, and L. Dritsas, "Coordination of Helicopter UAVs for Aerial Forest-Fire Surveillance," *Appl. Intell. Control to Eng. Syst.*, pp. 169–193, 2009, doi: 10.1007/978-90-481-3018-4_7.

[2] P. R. Ambati and R. Padhi, *A neuro-adaptive augmented dynamic inversion design for robust auto-landing*, vol. 19, no. 3. IFAC, 2014. doi: 10.3182/20140824-6-za-1003.01315.

[3] Z. Hou, P. Lu, and Z. Tu, "Nonsingular terminal sliding mode control for a quadrotor UAV with a total rotor failure," *Aerosp. Sci. Technol.*, vol. 98, p. 105716, 2020, doi: 10.1016/j.ast.2020.105716.

[4] R. Mori, K. Hirata, and T. Kinoshita, "Vision-based guidance control of a small-scale unmanned helicopter," *IEEE Int. Conf. Intell. Robot. Syst.*, pp. 2648–2653, 2007, doi: 10.1109/IROS.2007.4399623.

[5] K. Watanabe, Y. Iwatani, K. Nonaka, and K. Hashimoto, "A visual-servo-based assistant system for unmanned helicopter control," *2008 IEEE/RSJ Int. Conf. Intell. Robot. Syst. IROS*, pp. 822–827, 2008, doi: 10.1109/IROS.2008.4651153.

[6] S. Kumar and L. Dewan, "Different control scheme for the quadcopter: A Brief tour," *2020 1st IEEE Int. Conf. Meas. Instrumentation, Control Autom. ICMICA 2020*, 2020, doi: 10.1109/ICMICA48462.2020.9242886.

[7] T. Madani and A. Benallegue, *Adaptive Control via Backstepping Technique and Neural Networks of a Quadrotor Helicopter*, vol. 41, no. 2. IFAC, 2008. doi: 10.3182/20080706-5-kr-1001.01098.

[8] Z. Fang and X. Wang, "Design and Nonlinear Control of an Indoor Quadrotor Flying Robot *," pp. 429–434, 2010.

[9] A. W. A. Saif, M. Dhaifullah, M. Al-Malki, and M. El Shafie, "Modified backstepping control of Quadrotor," *Int. Multi-Conference Syst. Signals Devices, SSD 2012 - Summ. Proc.*, no. March, 2012, doi: 10.1109/SSD.2012.6197975.

[10] L. Fridman, J. A. Moreno, B. Bandyopadhyay, S. Kamal, and A. Chalanga, "Continuous nested algorithms: The fifth generation of sliding mode controllers," *Stud. Syst. Decis. Control*, vol. 24, pp. 5–35, 2015, doi: 10.1007/978-3-319-18290-2_2.

[11] Z. Jia, J. Yu, Y. Mei, Y. Chen, Y. Shen, and X. Ai, "Integral backstepping sliding mode control for quadrotor helicopter under external uncertain disturbances," *Aerosp. Sci. Technol.*, vol. 68, pp. 299–307, Sep. 2017, doi: 10.1016/J.AST.2017.05.022.

[12] J. J. Xiong, N. H. Guo, Y. X. Hong, and E. H. Zheng, "Improved Position and Attitude Tracking Control for a Quadrotor UAV," *Proc. - 2019 Chinese Autom. Congr. CAC 2019*, pp. 4197–4201, 2019, doi: 10.1109/CAC48633.2019.8996304.

[13] I. C. Dikmen, A. Arisoy, and H. Temeltaş, "Attitude control of a quadrotor," *RAST 2009 - Proc. 4th Int. Conf. Recent Adv. Sp. Technol.*, no. December 2015, pp. 722–727, 2009, doi: 10.1109/RAST.2009.5158286.

[14] X. Shi, Y. Cheng, C. Yin, S. Dadras, and X. Huang, "Design of Fractional-Order Backstepping Sliding Mode Control for Quadrotor UAV," *Asian J. Control*, vol. 21, no. 1, pp. 156–171, 2019, doi: 10.1002/asjc.1946.

[15] H. Le Nhu Ngoc Thanh and S. K. Hong, "Quadcopter robust adaptive second order sliding mode control based on PID sliding surface," *IEEE Access*, vol. 6, no. c, pp. 66850–66860, 2018, doi: 10.1109/ACCESS.2018.2877795.

[16] S. Kumar and L. Dewan, "PFOID-SMC approach to mitigate the effect of disturbance and parametric uncertainty on the quadcopter," *Int. J. Model. Identif. Control*, vol. 40, no. 4, p. 343, 2022, doi: 10.1504/IJMIC.2022.10050539.

[17] S. Kumar and L. Dewan, "Quadcopter stabilization using hybrid controller under mass variation and disturbances," *https://doi.org/10.1177/10775463221125628*, p. 107754632211256, Sep. 2022, doi: 10.1177/10775463221125628.

[18] H. Le Nhu Ngoc Thanh and S. K. Hong, "Quadcopter robust adaptive second order sliding mode control based on PID

sliding surface," *IEEE Access*, vol. 6, pp. 66850–66860, 2018, doi: 10.1109/ACCESS.2018.2877795.

[19] S. Bouabdallah and R. Siegwart, "Backstepping and sliding-mode techniques applied to an indoor micro Quadrotor," *Proc. - IEEE Int. Conf. Robot. Autom.*, vol. 2005, no. April, pp. 2247–2252, 2005, doi: 10.1109/ROBOT.2005.1570447.

[20] A. A. Mian and D. Wang, "Modeling and backstepping-based nonlinear control strategy for a 6 DOF quadrotor helicopter," *Chinese J. Aeronaut.*, vol. 21, no. 3, pp. 261–268, 2008, doi: 10.1016/S1000-9361(08)60034-5.

[21] K. Runcharoon and V. Srichatrapimuk, "Sliding Mode Control of quadrotor," *2013 Int. Conf. Technol. Adv. Electr. Electron. Comput. Eng. TAEECE 2013*, no. 1, pp. 552–557, 2013, doi: 10.1109/TAEECE.2013.6557334.

[22] Z. Fang, X. Y. Wang, and J. Sun, "Design and nonlinear control of an indoor quadrotor flying robot," *Proc. World Congr. Intell. Control Autom.*, pp. 429–434, 2010, doi: 10.1109/WCICA.2010.5553974.

[23] J. J. Xiong and E. H. Zheng, "Position and attitude tracking control for a quadrotor UAV," *ISA Trans.*, vol. 53, no. 3, pp. 725–731, 2014, doi: 10.1016/j.isatra.2014.01.004.

[24] I. Eker, "Second-order sliding mode control with experimental application," *ISA Trans.*, vol. 49, no. 3, pp. 394–405, 2010, doi: 10.1016/j.isatra.2010.03.010.